HHS Public Access

Author manuscript

Nat Chem. Author manuscript; available in PMC 2018 August 01.

Published in final edited form as:

Nat Chem. 2018 August ; 10(8): 873–880. doi:10.1038/s41557-018-0068-x.

A human MUTYH variant linking colonic polyposis to redox degradation of the $[4Fe4S]^{2+}$ cluster

Kevin J. McDonnell[1], **Joseph A. Chemler**[2], **Phillip L. Bartels**[3], **Elizabeth O'Brien**[3], **Monica L. Marvin**[4], **Janice Ortega**[5], **Ralph H. Stern**[6], **Leon Raskin**[7], **GuoMin Li**[5], **David H. Sherman**[2,8], **Jacqueline K. Barton**[3], and **Stephen B. Gruber**[1]

[1]University of Southern California Norris Comprehensive Cancer Center, Los Angeles, CA, USA

[2]Life Sciences Institute, University of Michigan, Ann Arbor, MI, USA

[3]Division of Chemistry and Chemical Engineering, California Institute of Technology, Pasadena, CA, USA

[4]Department of Human Genetics, University of Michigan, Ann Arbor, MI, USA

[5]Department of Radiation Oncology, University of Texas Southwestern Medical Center, Dallas, TX, USA

[6]Division of Molecular Medicine and Genetics, Department of Internal Medicine, University of Michigan, Ann Arbor, MI, USA

[7]Amgen Inc., Thousand Oaks, CA, USA

[8]Departments of Medicinal Chemistry, Chemistry and Microbiology & Immunology, University of Michigan, Ann Arbor, MI, USA

Abstract

The human DNA repair enzyme MUTYH excises mispaired adenine residues in oxidized DNA. Homozygous *MUTYH* mutations underlie the autosomal, recessive cancer syndrome *MUTYH* associated polyposis. We report a MUTYH variant, p.C306W (c.918C>G), with a tryptophan residue in place of native cysteine, that ligates the [4Fe4S] cluster in a patient with colonic polyposis and family history of earlyage colon cancer. In bacterial MutY, the [4Fe4S] cluster is redox active, allowing rapid localization to target lesions by longrange, DNAmediated signalling. In the current study, using DNA electrochemistry, we determine that wildtype MUTYH is similarly redoxactive, but MUTYH C306W undergoes rapid oxidative degradation of its cluster to

Correspondence to: David H. Sherman; Jacqueline K. Barton; Stephen B. Gruber.

These authors wish it to be known that, in their opinion, the first 3 authors should be regarded as joint First Authors: Kevin J. McDonnell, Joseph A. Chemler, Phillip L. Bartels.

Electronic supplementary material

Supplementary information is available for this paper at https://doi.org/10.1038/s415570180068x.

Author contributions

K.M., J.C., P.B., E.O., D.S., J.B. and S.G. conceived and designed the experiments. K.M., J.C. and P.B. cowrote the paper with input from all authors. R.S., L.R., M.M., J.O. and G.L. contributed materials and analysis tools. K.M., J.C. and P.B. performed the experiments.

Competing interests The authors declare no competing interests.

[3Fe4S]$^{+}$, with loss of redox signalling. In MUTYH C306W, oxidative cluster degradation leads to decreased DNA binding and enzyme function. This study confirms redox activity in eukaryotic DNA repair proteins and establishes MUTYH C306W as a pathogenic variant, highlighting the essential role of redox signalling by the [4Fe4S] cluster.

Graphical abstract

The [4Fe4S]$^{2+}$ clustercontaining DNArepair enzyme MUTYH helps safeguard the integrity of Watson–Crick base pairing and the human genetic code. The MUTYH [4Fe4S]$^{2+}$ cluster mediates DNA redox signalling and DNA lesion identification. Now, a MUTYH pathologic variant associated with catastrophic [4Fe4S]$^{2+}$ cluster redox degradation, impairment of DNA signalling and human colonic tumorigenesis has been identified.

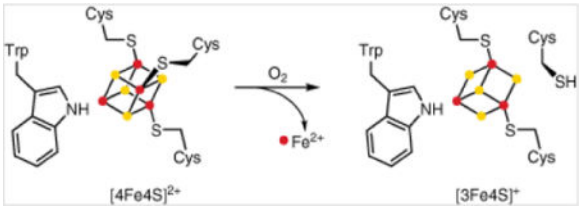

In cells sustaining oxidative damage, genomic guanine residues are frequently oxidized to 8-oxo7,8dihydroguanine (8oxoG). Unlike guanine, 8oxoG can pair effectively with either cytosine or adenine bases, with potentially serious mutagenic consequences[1]. A DNA glycosylase conserved among species from bacteria to humans, known in humans as MUTYH, removes adenine from these 8oxoG:A mispairs as part of the base excision repair pathway. In humans, germline *MUTYH* mutations that impair enzymatic activity lead to an increase in G:C>T:A transversions that have been shown to result in missense mutations in the *APC* tumour suppressor gene in epithelial cells lining the colon. Mutations in *APC* are the first recognizable genetic events that initiate malignant transformation of normal colonic epithelia into polyps, specifically adenomas, before the acquisition of other mutations that complete the neoplastic conversion sequence from normal tissue through adenoma to carcinoma[2]. Biallelic mutations of *MUTYH* give rise to the autosomal recessive cancer genetic syndrome, *MUTYH*associated polyposis (MAP)[3]. Typically, by their fifth decade, MAP patients develop 10–100 colonic polyps[4]. *MUTYH* variants are common, with a prevalence of at least 1–2% among western Europeans[5], and the colorectal cancer risk increases nearly 2 and 100fold for mono and biallelic *MUTYH* mutations, respectively[6].

The MUTYH protein comprises three major regions[7]: the N terminus, which contains the endonuclease III sixhelix barrel catalytic domain, the interdomain connector (IDC) and the C terminus, corresponding to protein residues 1–306, 315–366 and 368–500, respectively. The MUTYH N terminus contains a [4Fe4S]$^{2+}$ cluster ligated by four cysteine residues; although metabolically expensive, the cluster is conserved in MutY homologues across all domains of life[8]. A rare exception is the yeast endonuclease III homologue Ntg1, which has no cluster, but one is present in a second yeast homologue (Ntg2)[9]. Indeed, the only organisms lacking a cluster in any MutY homologue are specialized anaerobes subject to lower levels of oxidative stress[10]. Studies performed on *Escherichia coli* MutY and its

homologue endonuclease III (EndoIII) have demonstrated that the cluster is unnecessary for structural integrity and is largely redoxinert in solution[11, 12]. However, when *E. coli* MutY and EndoIII were incubated on duplex DNAmodified gold electrodes, a reversible redox signal centred near 80mV versus normal hydrogen electrode (NHE) was observed for both proteins, and was identified as the $[4Fe4S]^{3+/2+}$ couple, an assignment supported by electron paramagnetic resonance (EPR) spectroscopy[13]. Subsequent experiments with EndoIII on a graphite electrode in the presence and absence of DNA revealed that binding to the negatively charged DNA backbone shifts the redox potential of these proteins by about −200mV, activating the cluster towards oxidation and resulting in a significant increase in binding affinity of the oxidized $[4Fe4S]^{3+}$ form of the enzyme relative to the native $[4Fe4S]^{2+}$ form[14].

These studies have led to a model in which [4Fe4S] base excision repair (BER) proteins with similar DNAbound redox potentials use reversible redox exchanges to signal to one another across the genome, taking advantage of the unique ability of DNA to conduct charge across the πstacked base pairs (bps) in a process known as DNAmediated charge transport (DNA CT)[15, 16]. DNA CT has both a very shallow distance dependence and an exquisite sensitivity to even slight disruptions in base pair stacking, making it an ideal lesion reporter. In our CT signalling model, oxidative stress generates highly reactive species, such as guanine radicals, which can then oxidize proteins including MutY[17]. If another [4Fe4S] protein is bound at a distal site and the intervening DNA is undamaged, it can send an electron through the DNA to reduce the first protein. Following reduction, the protein's affinity for DNA is decreased and the protein dissociates to another region of the genome, while the oxidized protein remains bound. In the presence of a lesion, DNA CT is impaired, and the oxidized protein will remain bound and diffuse towards the site of damage. Thus, DNA CT constitutes a means for [4Fe4S] proteins to scan a vast genome on a relevant timescale and redistribute in the vicinity of lesions. In the case of *E. coli*, longrange signalling by DNA CT has been estimated to reduce the damage search time from 45min to 10min or less[18].

In the present study, we describe a novel MUTYH variant, p.C306W, identified in a patient exhibiting colonic polyposis. Using an *E. coli* overexpression system, this variant was generated together with wildtype (WT) MUTYH and the wellcharacterized pathologic variants Y179C and G396D. We used electrochemistry, UV–vis and EPR spectroscopy to compare the redox properties of these four MUTYH variants. Enzymatic activity and DNA binding parameters were determined using glycosylase assays and biolayer interferometry (BLI), respectively. Together, these results provide strong evidence for a primary function of the [4Fe4S] cluster in DNAmediated redox signalling and establish MUTYH C306W as a pathogenic variant, enhancing our understanding of the role of the [4Fe4S] cluster in human disease.

Results

Identification and functional deficiencies of a novel MUTYH variant

A novel germline *MUTYH* variant, c.918C>G (p.C306W), together with the previously well-described *MUTYH* mutation c.1187G>A (p.G396D), were identified in a patient with

colonic polyposis whose family history was significant for earlyage colon cancer. The cysteine at position 306 represents one of the four cysteine residues that mediate integration of the conserved MUTYH [4Fe4S] cluster. In bacterial MutY, cluster loss is associated with decreased protein function[12], which suggests that in MUTYH the C306W variant may affect the integrity of the [4Fe4S] cluster and represent a pathologic mutant (Fig. 1a illustrates the structure of bacterial MutY and identifies corresponding residues in MUTYH).

Supporting the potential pathogenicity of the novel ~918C>G variant, we established that this variant is situated in a trans chromosomal configuration relative to the ~1187G>A *MUTYH* mutation (Supplementary Fig. 1). Further evidence of the pathogenic nature of the ~918C>G variant was apparent in the sequence of the *APC* gene in somatic DNA originating from a colonic adenoma from the patient. This sequencing revealed the presence of a G:C>T:A transversion in the *APC* gene, which is the hallmark genetic lesion indicative of deficient *MUTYH*mediated DNA enzymatic repair[2] (Supplementary Fig. 2).

Four MUTYH proteins (WT, the wellcharacterized mutants G396D and Y179C, and the novel variant C306W) were overexpressed in *E. coli* and purified by nickel affinity chromatography. Monomeric MUTYH proteins were produced by treatment with 20mM β-mercaptoethanol, followed by size exclusion fast protein liquid chromatography with validation by UV spectroscopy (Supplementary Figs. 3 and 4). Relative to WT MUTYH, G396D MUTYH demonstrated a significant decrease in glycosylase activity and Y179C a severe deficiency；comparative assessment of C306W MUTYH revealed a virtual absence of activity, thus establishing its pathogenicity (Fig. 1b). The glycosylase activities of aggregated MUTYH proteins were also assessed；in these experiments C306W was similarly deficient in glycosylase activity (Supplementary Fig. 5).

For a more complete functional comparison of the four MUTYH variants, we conducted timecourse glycosylase assays under multiple turnover conditions in order to quantitatively determine the proportion of active enzyme in each sample[19, 20, 21]. These assays were performed using dsDNA containing an 8oxoG:A mispair together with varying concentrations of MUTYH proteins. The experimental results demonstrate an initial burst of adenine excision activity proportional to the active fraction, A_0, of the protein sample (Fig. 1c and Table 1). The excision reaction rate constants, k_B and k_L, were determined for the exponential and linear phases of the reaction, respectively (Table 1). Both WT MUTYH and G396D proteins had comparable linear rates for turnover and the highest fraction of active protein. In contrast, the C306W MUTYH mutant was essentially devoid of adenine excision activity and Y179C had no detectable turnover. The fractions of active MUTYH were then used to correct for the total amount of protein used in the glycosylase assay (Fig. 2d), confirming that WT MUTYH and G396D mutant had comparable activities, while C306W and Y179C mutants displayed poor activity. The poor activity observed in MUTYH C306W could have two possible explanations: either that this mutant was catalytically inactive or it was unable to bind specifically to DNA (as is the case with low activity in the weakly bound Y179C).

To help distinguish between these possibilities, we used BLI[22] to measure the binding parameters of the MUTYH proteins. We compared the binding of WT MUTYH and the

G396D, Y179C and C306W mutants to DNA containing an 8oxoG:A mispaired duplex. Table 1 summarizes the binding kinetics. Relative to WT MUTYH, the G396D and Y179C variants demonstrated increasing values of K_D primarily due to decreased association rates. There was no detectable binding for the C306W mutant within the protein concentration range tested, suggesting that the low activity levels observed in this mutant were due primarily to ineffective DNA binding.

Together, these data demonstrate the functional deficiency and establish the pathogenicity of the C306W MUTYH variant. In bacterial MutY, [4Fe4S] cluster loss is associated with decreased protein function[12], which suggests that in MUTYH the C306W variant may affect the integrity of the [4Fe4S] cluster, accounting for the pathogenicity of this mutant.

To assess the integrity of the [4Fe4S] cluster, iron loading of the clusters of WT MUTYH and mutants Y179C, G396D and C306W were compared by quantifying the iron present in each sample using inductively coupled plasma–highresolution mass spectrometry (ICP-HRMS) for elemental analysis[23]. Consistent with disruption of the Fe–S cluster loop in the C306W variant, this protein exhibited substantially lower iron content relative to the other MUTYH proteins tested (Table 2). However, UV–vis spectra taken from disrupted aggregates of all four variants distinctly showed the broad peak centred at 410nm that is characteristic of a [4Fe4S] cluster, indicating that MUTYH C306W is still capable of binding an intact cluster and further suggesting that loading by cellular machinery is still effective (Supplementary Fig. 6). In addition, circular dichroism (CD) spectra of WT MUTYH and the C306W mutant were indistinguishable, confirming that no global conformational changes were induced by this mutation (Supplementary Fig. 6). Thus, the low cluster content, as measured by ICPHRMS, was instead tentatively associated with decreased protein stability in this mutant, and subsequent electrochemical and EPR experiments were used to more reliably examine the [4Fe4S] cluster properties in detail.

DNA-bound electrochemistry of WT and mutant MUTYH

Having observed that MUTYH C306W appeared to incorporate less iron despite its capacity to bind an intact cluster, we next assessed its redox properties on DNAmodified gold electrodes alongside WT, G396D and Y179C MUTYH (Fig. 2). We reasoned that electrochemical analysis would aid these studies for two reasons: first, access to highly purified WT MUTYH allowed us to determine if the human protein behaved in a manner similar to its bacterial counterpart, and, second, electrochemical monitoring would provide an effective way to assess the stability of MUTYH C306W over time. Specifically, we expected that the predicted instability of MUTYH C306W would result in electrochemical signals that were either smaller than WT or less stable over time.

In these experiments, MUTYH was incubated in storage buffer (20mM Tris, pH7.4, 100mM NaCl, 1mM DTT, 10% glycerol vol/vol) and periodically scanned by cyclic voltammetry (CV) and square wave voltammetry (SQWV). Aggregated protein preparations were treated with 20mM βmercaptoethanol and exchanged into storage buffer with fresh DTT immediately before electrochemical analysis. UV–vis spectroscopy confirmed that treated proteins were monomeric and contained intact [4Fe4S] clusters. Notably, cluster loading in monomeric WT MUTYH prepared from disassembled aggregates was significantly lower

than expected (~15% as determined from the A_{410}:A_{280} ratio), but the low loading actually turned out to be advantageous for these experiments. Because apoproteins may bind some available DNA on the surface and thus decrease signal amplitude, the most important factor in making direct comparisons between different MUTYH proteins on an electrode is not absolute loading (although high levels are ideal) but that each variant is similarly loaded with a [4Fe4S] cluster. Fortunately, this turned out to be the case, with the MUTYH C306W samples also ~15% loaded as determined by UV–vis spectroscopy (Supplementary Fig. 6).

To test multiple conditions simultaneously, DNA monolayers were prepared on multiplexed gold electrodes, which enabled up to four experiments to be conducted in parallel[24]. In this case, half of the available quadrants consisted of unmodified well matched (WM) DNA and half of substrate trap FA:OG DNA, which was included in an effort to enhance the signal amplitude by increasing the DNA binding affinity. In addition, both highdensity (formed in the presence of 100mM $MgCl_2$) and lowdensity monolayers were compared on a single chip. DNA surface density is an important parameter for protein experiments[24]: highdensity films have more DNA on the surface (30–50pmol/cm^{-2}), which can improve DNAmediated signalling by sterically hindering large proteins, while lowdensity films contain less DNA (15–20pmolcm^{-2}), which can be more readily accessible to proteins[25, 26]. Overall, the effect of each type of film is likely to depend strongly on the particular protein being studied, and both have been used in previous studies[24].

In the case of WT MUTYH at a concentration of ~2.5μM [4Fe4S] cluster, a reversible redox signal with a midpoint potential of 106±1mV versus NHE was immediately apparent, and increased over the course of the experiment (Fig. 3). The midpoint potential was similar to the 65–95mV (versus NHE) range reported for other [4Fe4S] proteins bound to DNA, with the slightly higher potential of MUTYH most probably attributable to the distinct buffer conditions. Although the signals were relatively small, they were readily quantifiable: on lowdensity films containing WM DNA, CV peak areas were $31\pm1\times10^{-2}$ nC for the reductive peak and $-33\pm2\times10^{-2}$ nC for the oxidative peak, while the equivalent values on highdensity films were $25\pm2\times10^{-2}$ nC and $-27\pm3\times10^{-2}$ nC, respectively. Interestingly, no significant differences in signal intensity were observed between WM and FA:OG DNA, with CV reductive and oxidative peak charges of $28\pm1\times10^{-2}$ nC and $-34\pm4\times10^{-2}$ nC on lowdensity FA:OG DNA films and $24\pm2\times10^{-2}$ nC and $-24\pm 1\times10^{-2}$ nC on highdensity films. The FA:OG substrate trap is known to increase the binding affinity of the very similar murine Mutyh on a 30mer duplex by an order of magnitude[27], and the absence of any clear change in signal intensity suggests that our system is not sufficiently sensitive to detect this difference. Several possible explanations exist for this insensitivity. First, it may be that the absolute amount of accessible DNA on either surface is too low to detect a difference between WM and FA:OG substrates. Alternatively, the significant amount of apoprotein present may have blocked some of the accessible DNA from fully loaded protein. A further complicating factor may be the presence of DNA tethered to a surface rather than in solution, which might lower the chances of protein encounter. Despite these potential limitations, we were able to definitively observe and quantify signals from DNAbound MUTYH.

The signal from MUTYH C306W (also at the ~2.5μM [4Fe4S] cluster) was comparable in both potential and maximum size to WT, although the signal size was considerably more variable between experiments. Although it was not clearly CTdeficient, as might have been expected, the C306W signal decreased in size at a steady rate after 1–2h of incubation, consistent with the loss of iron seen by ICPHRMS. In addition, the intensity of a second, irreversible peak centred around −50mV versus NHE increased as the reversible $[4Fe4S]^{3+/2+}$ signal decayed. This secondary peak was unprecedented among BER proteins on DNAmodified electrodes, but its growth in parallel with loss of the reversible signal suggested that it was some form of degradation product.

Although all of the DNAprocessing enzymes studied thus far have shown stabilization of the $[4Fe4S]^{3+}$ form on DNA binding to yield a reversible $[4Fe4S]^{3+/2+}$ signal on an electrode, loss of iron by the oxidized $[4Fe4S]^{3+}$ species to form the $[3Fe4S]^{+}$ cluster has been reported in bacterial MutY and EndoIII when the samples were frozen for EPR under aerobic conditions[13]. As this is the first step in cluster degradation, we considered the [3Fe4S] cluster to be a likely candidate for the identity of this unexpected MUTYH C306W species. At approximately −50mV versus NHE, the MUTYH C306W secondary peak fell within the range of reported $[3Fe4S]^{+}$ cluster potentials[28], supporting assignment to this species. The irreversible nature of the signal was unusual, given that [3Fe4S] clusters can typically access a reversible $1^{+}/0$ redox couple, but, given the significant effect of even a single unit of cluster charge on DNA binding affinity[14], irreversibility could be explained as protein dissociation from DNA on reduction to the neutral $[3Fe4S]^{0}$ cluster.

Confirming that the [4Fe4S] cluster degradation observed in MUTYH C306W was unique to this mutant, electrochemical analysis of DNAbound Y179C and G396D (both 2.5μM in storage buffer) yielded reversible signals at nearly the same potential as WT with no secondary peak present (Table 3). Like WT, the signals from both of these variants increased over time and remained stable for several hours (Fig. 3). Notably, the Y179C signal was only about half as large as that for the WT, which is consistent with the reported lower binding affinity of this mutant relative to both WT and G396D (7.5nM for Y179C versus 2.2 and 4.9nM for WT and G396D, respectively)[19]. Overall, however, both mutants were more similar to WT than C306W in their redox properties, which was unsurprising given that the cluster in these variants is unaltered. The propensity for the MUTYH C306W cluster to degrade by redox activity provides a possible explanation for the low DNAbinding affinity observed with BLI binding studies, as previous MutY studies have demonstrated that apoprotein lacking cluster remains structurally intact, but exhibits defective DNA binding[12].

Characterization of the C306W degradation product

In an effort to characterize the MUTYH C306W cluster degradation product more fully, we proceeded to assess its dependence on oxygen, which is often involved in $[3Fe4S]^{+}$ cluster formation[13]. Specifically, we employed electrochemical and UV–vis spectroscopic analysis to compare aerobically oxidized proteins with those maintained in an anaerobic environment. For an effective comparison, a single C306W sample was concentrated and one half of the sample was diluted to 2.5μM in degassed buffer and placed on a chip

containing lowdensity WM DNA in an anaerobic glove bag (95% N_2/5% H_2 atmosphere), while the other half was maintained in aerobic conditions and oxidized on a DNAmodified gold rod electrode held at 0.412 V versus NHE. The anaerobic sample was scanned periodically by CV and SQWV, and, following electrolysis, the oxidized sample was transferred to the glove bag and added to a separate quadrant on the same chip. In addition to electrochemistry, UV–vis spectra were recorded before and after electrolysis both to observe changes in the 410nm peak and to ensure that the oxidized sample did not aggregate.

Quantification of the total charge passed during electrolysis indicated nearcomplete oxidation of the aerobic protein by ~60min. Before electrolysis, the UV–vis spectrum showed the broad peak centered at 410nm characteristic of a [4Fe4S] cluster, but, after oxidation, the absorbance increased over a broad range from 700 to 300nm, with a poorly defined peak around 410nm and a substantial shoulder between 400 and 300nm (Fig. 3). Such absorbance features are a general characteristic of cluster oxidation, although UV–vis spectra alone are insufficient to precisely identify the oxidized species generated[29]. Importantly, the 280nm peak remained sharp and distinct even after oxidation, and the spectrum was not elevated at 800nm, demonstrating that the protein had not aggregated and confirming that all changes were due solely to cluster oxidation. This result stands in stark contrast to the soluble MUTYH aggregates observed in both WT and C306W in the absence of DTT, which were visibly cloudy with a Ushaped UV–vis spectrum characteristic of aggregation, highly elevated absorbance at 800nm, no distinct [4Fe4S] peak, and a very slight 280nm peak visible only as a shoulder (Supplementary Fig. 6).

CV of the aerobically oxidized C306W MUTYH variant revealed an irreversible peak comparable in size to the main reversible peaks; in contrast, the equivalent peak in the anaerobic sample was much smaller than the main peak and had not changed from initial levels (Fig. 3). Furthermore, the reversible signal of the anaerobic sample increased over time and exceeded even the strongest signals observed for aerobically incubated WT MUTYH, which was even more intriguing given that the anaerobic sample had been incubating on the electrode for several hours. Supporting greater instability of the C306W [4Fe4S] cluster, aerobic oxidation of WT MUTYH gave low bulk electrolysis yields, and no readily apparent irreversible peak was present by CV. In addition, the UV–vis spectra of WT before and after oxidation were indistinguishable. Taken together, the apparent sensitivity of MUTYH C306W to oxidation and degradation in air along with the absence of any observable degradation in aerobically oxidized WT MUTYH supported the assignment of the secondary peak to a $[3Fe4S]^+$ cluster, although these techniques alone could not verify this identity.

EPR spectroscopy of MUTYH

Having confirmed that the C306W degradation product was an oxidized species forming under aerobic conditions, we turned to EPR spectroscopy as a final step towards its definitive identification. EPR provides a means of distinguishing among different paramagnetic species and is commonly used to study Fe–S proteins[28, 29, 30]. Although EPR analysis can be very informative, there were two general concerns with respect to MUTYH. First, EPR experiments are generally performed with significantly higher levels of

concentrated protein than those used in our electrochemical experiments with MUTYH: signals have been reported for 10μM *E. coli* EndoIII[13] and ~9μM DNA polymerase δ (ref. [31]), but even these were still three to four times more concentrated than the MUTYH samples. Second, the low temperatures necessary to resolve signals from [4Fe4S] clusters (10–35K) require the samples to be frozen before analysis, which can impact protein stability if the buffer pH changes with temperature, as is the case for the Tris buffers used in our MUTYH studies[32].

Therefore, before attempting EPR, all MUTYH variants were concentrated and exchanged into a HEPES buffer (20mM HEPES, pH7.4, 100mM KCl, 1mM DTT, 10% glycerol vol/vol, pH7.4), and potassium was used in place of sodium as a further precaution to stabilize the pH at low temperature[33]. UV–vis spectroscopy and electrochemistry (Supplementary Fig. 6; for details see Supplementary Section VIII) were used to confirm protein stability in HEPES and to verify that the redox properties remained comparable. As observed in the UV–vis spectra (Fig. 3), all MUTYH variants maintained their monomeric form in this buffer, although they could not be concentrated beyond 15μM without forming soluble aggregates. When such aggregates did form, they were readily resolved by simple dilution, and the UV–vis spectra of WT MUTYH and mutants Y179C and G396D all retained a sharp 410nm peak with ~15% cluster loading even after an additional freeze–thaw cycle one week after buffer exchange (Fig. 3). In contrast, the spectrum of the MUTYH C306W protein closely resembled the aerobically oxidized sample described previously (Fig. 3). Oxidation may have occurred over the extended aerobic buffer exchange process or during the freeze–thaw cycle on the day of EPR experiments. Because the extinction coefficient at 410nm was unknown for the MUTYH C306W product, we estimated cluster loading in this mutant by comparing the magnitude of absorbance with the earlier aerobically oxidized sample, yielding a concentration comparable to the other variants.

All EPR spectra of MUTYH proteins were obtained with 15μM WT and C306W and 5μM G396D and Y179C (the latter mutants were not available in larger amounts). From the broadened UV–vis absorption, we predicted that the corresponding EPR spectrum would show evidence of either the $[3Fe4S]^{+}$ cluster or a more advanced degradation product, while WT, Y179C and G396D were expected to be diamagnetic and thus EPR silent. Unexpectedly, all of the samples showed a small, broad signal with a shoulder at g=2.04 (Fig. 3) most likely attributable to oxidation during the aerobic freezing process, as reported previously for *E. coli* EndoIII and MutY. Nonetheless, MUTYH C306W protein displayed a much sharper signal with a clear peak centred at g=2.018 (Fig. 3), which is characteristic of $[3Fe4S]^{+}$ clusters[28, 30]. Importantly, the C306W EPR signal, but not the broad signals of WT and the other MUTYH variants, closely resembled spectra from chemically oxidized *E. coli* EndoIII and MutY that were also assigned to the $[3Fe4S]^{+}$ cluster[13]. Although some of the C306W [4Fe4S] degradation may have occurred during sample freezing, the significantly larger and sharper EPR signal relative to the other variants, coupled with the UV–vis spectrum indicating previous oxidation, contradict this notion.

Discussion

In the present study we describe a novel MUTYH variant, C306W, and its association with the development of colonic polyposis and a family history of colon cancer. We determined that the C306W variant lacks DNA abscission activity and has decreased ability to bind target DNA, establishing the pathogenicity of this variant. In C306W MUTYH there is loss of a cysteine residue that ligates the MUTYH [4Fe4S] cluster. This finding raised the possibility that the loss of the cysteine might disrupt the integrity of the [4Fe4S] cluster and provide an explanation for the pathogenicity associated with MUTYH C306W. The observation by ICPHRMS that the [4Fe4S] cluster of C306W exhibits significantly lower iron content further bolstered this hypothesis and prompted an electrochemical, mechanistic investigation of the MUTYH [4Fe4S] cluster and the effect of cysteine loss in the C306W variant.

Towards this end, we present direct evidence of redox signalling in eukaryotic MUTYH. DNAmodified electrochemical analysis revealed the redox potentials of all MUTYH variants studied to be in general agreement with earlier work (Table 3), with the potentials as measured in HEPES buffer almost identical to those obtained for *E. coli* MutY in phosphate buffer[13]. The similarity of the WT MUTYH electrochemical signals to those of the *E. coli* protein strongly supports the notion that the primary function of the conserved [4Fe4S] cluster is redox activity in all organisms. Furthermore, the DNAmediated nature of this signal in MUTYH suggests that a process akin to the DNAmediated redoxbased damage search observed in bacteria may also be present and operating in humans.

Unlike WT MUTYH, the C306W mutant showed an unexpected, and irreversible, reduction between −50 and −100mV versus NHE, in combination with loss of the reversible signal at ~100mV versus NHE; EPR spectroscopy confirmed this additional signal to be the $[3Fe4S]^{+/0}$ couple. The observed degradation and poor DNA binding in MUTYH C306W are consistent with the higher DNA binding affinity associated with increasing charge in [4Fe4S] clusters, in which coulombic effects cause the $[4Fe4S]^{3+}$ cluster to bind the DNA polyanion significantly more tightly than the $[4Fe4S]^{2+}$ form[14]. The relationship of cluster charge to binding affinity predicts that the $[3Fe4S]^{+}$ and $[3Fe4S]^{0}$ degradation products, with one and zero net charges, would bind much more weakly to DNA than the $[4Fe4S]^{2+}$ form, consistent with the irreversible reduction observed in degraded MUTYH C306W. Overall, our results suggest that, for MUTYH C306W, ordinary redox activity on DNA would lead to oxidation to the $[4Fe4S]^{3+}$ state, as is typical in these proteins, but the lower stability of the cluster would promote the loss of an iron atom and irreversible dissociation following a second redox signalling cycle. Ultimately, this process could result in the low iron content measured by ICPHRMS, an effect that might well be exacerbated if the dissociated $[3Fe4S]^{0}$ form degraded further when removed from the protective environment of DNA. Cluster degradation in MUTYH C306W is also consistent with the low levels of glycosylase activity and poor DNA binding affinity as measured by BLI (Table 1), which are attributes of bacterial MutY following cluster removal[12]. This inherent instability of the C306W [4Fe4S] cluster and consequent loss of function we propose to be a source of pathogenicity in this MUTYH variant.

With regard to other potential sources of pathogenicity, we recognize that MUTYH is also regulated by posttranslational modifications, including phosphorylation and ubiquitination, that could be altered by this mutation[34, 35]. However, these sites are in different regions of the protein relative to the [4Fe4S] domain, and are thus unlikely to be affected by this particular mutation. Thus, redoxstimulated cluster degradation is most likely the primary cause of pathogenicity in MUTYH C306W.

The irreversible [3Fe4S] cluster signal seen in MUTYH C306W has not been observed previously in electrochemical studies of DNAprocessing [4Fe4S] proteins, but the signal was within the same redox potential range reported for the $[3Fe4S]^{+/0}$ couple of bacterial Ni–Fe hydrogenase and fumarate reductase enzymes[36, 37]. In *E. coli* MutY, [4Fe4S] cluster ligand substitution of the corresponding cysteine residue has been shown to be defective in DNA binding, similar to the situation with MUTYH C306W[38]. We note, however, that none of the substitutions involving *E. coli* MutY occurred with a residue as bulky as tryptophan[38].

Given the results obtained for MUTYH C306W, it appears probable that mutations in other residues that alter the region around the [4Fe4S] cluster will be similarly deficient in their ability to mediate repair of oxidatively damaged DNA *in vivo*[39, 40, 41, 42, 43]. Indeed, both germline and somatic alterations in other cysteines comprising the [4Fe4S] cluster and the four arginines that participate in hydrogen bonding to the cysteines coordinating the cluster[44] (Supplementary Tables 1 and 2) have been identified and are associated with colorectal as well as other cancers[7]. It is probable that these mutations also result in instability, degradation and dysfunction of the [4Fe4S] cluster secondary to the same mechanisms detailed above. The effects of these lesions as well as the C306W variant underscore the importance of the [4Fe4S] cofactor in establishing competent MUTYH-mediated DNA repair.

The current study advances our basic electrochemical understanding of the redox chemistry, function and integrity of the [4Fe4S] cluster, as well as providing insight into the pathologic sequelae resulting from disruption of the cluster. Specifically, we have documented and provided an explanation for a novel mechanism of colonic polyposis and cancer predisposition linked to electrochemical compromise of the MUTYH [4Fe4S] cluster. Future studies, we anticipate, will provide additional clarification of the central role of the [4Fe4S] cluster in MUTYHmediated DNA repair and its underlying electrochemistry.

Reporting Summary

Further information on experimental design is available in the Nature Research Reporting Summary linked to this article.

Data availability

The data sets generated during and/or analysed during the current study are available from the corresponding author.

Supplementary Material

Refer to Web version on PubMed Central for supplementary material.

Acknowledgments

The authors thank T. Huston of the W.M. Keck Lab in the Department of Earth & Environmental Sciences at the University of Michigan for ICPHRMS analyses. This work was funded in part by a Ruth L. Kirschstein National Research Service Award (GM095065 to J.A.C.), a National Institutes of Health (NIH) grant (R35 GM118101) and an H.W. Vahlteich Professorship (to D.H.S.), a Ruth L. Kirschstein National Research Service Award and American Society of Clinical Oncology Young Investigator Award (to K.M.), grant 1R01CA197350 (to S.B.G.), a USC Norris Comprehensive Cancer Center Support Grant (CA014089 to S.B.G.), an award from the Ming Hsieh Institute for Engineering—Medicine for Cancer, and support from Daniel and Maryann Fong and the Anton B. Burg Foundation (to S.B.G.). P.L.B., E.O.B. and J.K.B. acknowledge the NIH (GM126904 to J.K.B.) and Moore Foundation for financial support. E.O.B. acknowledges NIH training grant T32GM07616 and a Ralph Parsons Fellowship for support.

References

1. Markkanen E, Dorn J, Hubscher U. MUTYH DNA glycosylase: the rationale for removing undamaged bases from the DNA. Front Genet. 2013; 4:18. [PubMed: 23450852]
2. AlTassan N, et al. Inherited variants of MYH associated with somatic G:C→T:A mutations in colorectal tumors. Nat Genet. 2002; 30:227–232. [PubMed: 11818965]
3. Sampson JR, et al. Autosomal recessive colorectal adenomatous polyposis due to inherited mutations of MYH. Lancet. 2003; 362:39–41. [PubMed: 12853198]
4. Sieber OM, et al. Multiple colorectal adenomas, classic adenomatous polyposis, and germline mutations in MYH. N Engl J Med. 2003; 348:791–799. [PubMed: 12606733]
5. Cleary SP, et al. Germline MutY human homologue mutations and colorectal cancer: a multisite case–control study. Gastroenterology. 2009; 136:1251–1260. [PubMed: 19245865]
6. Jones N, et al. Increased colorectal cancer incidence in obligate carriers of heterozygous mutations in MUTYH. Gastroenterology. 2009; 137:489–494. [PubMed: 19394335]
7. Out AA, et al. Leiden Open Variation Database of the MUTYH gene. Human Mutat. 2010; 31:1205–1215.
8. Maio N, Rouault TA. Iron–sulfur cluster biogenesis in mammalian cells: new insights into the molecular mechanisms of cluster delivery. Biochim Biophys Acta. 2015; 1853:1493–1512. [PubMed: 25245479]
9. Alseth I, et al. The *Saccharomyces cerevisiae* homologues of endonuclease III from *Escherichia coli*, Ntg1 and Ntg2, are both required for efficient repair of spontaneous and induced oxidative DNA damage in yeast. Mol Cell Biol. 1999; 19:3779–3787. [PubMed: 10207101]
10. TrasvinaArenas CH, LopezCastillo LM, SanchezSandoval E, Brieba LG. Dispensability of the [4Fe4S] cluster in novel homologues of adenine glycosylase MutY. FEBS J. 2016; 283:521–540. [PubMed: 26613369]
11. Cunningham RP, et al. Endonuclease III is an iron–sulfur protein. Biochemistry. 1989; 28:4450–4455. [PubMed: 2548577]
12. Porello SL, Cannon MJ, David SS. A substrate recognition role for the $[4Fe4S]^{2+}$ cluster of the DNA repair glycosylase MutY. Biochemistry. 1998; 37:6465–6475. [PubMed: 9572864]
13. Boal AK, et al. DNAbound redox activity of DNA repair glycosylases containing [4Fe4S] clusters. Biochemistry. 2005; 44:8397–8407. [PubMed: 15938629]
14. Gorodetsky AA, Boal AK, Barton JK. Direct electrochemistry of endonuclease III in the presence and absence of DNA. J Am Chem Soc. 2006; 128:12082–12083. [PubMed: 16967954]
15. Arnold AR, Grodick MA, Barton JK. DNA charge transport: from chemical principles to the cell. Cell Chem Biol. 2016; 23:183–197. [PubMed: 26933744]
16. O'Brien E, Silva RM, Barton JK. Redox signaling through DNA. Isr J Chem. 2016; 56:705–723. [PubMed: 28090121]

17. Yavin E, et al. Protein–DNA charge transport: redox activation of a DNA repair protein by guanine radical. Proc Natl Acad Sci USA. 2005; 102:3546–3551. [PubMed: 15738421]
18. Boal AK, et al. Redox signaling between DNA repair proteins for efficient lesion detection. Proc Natl Acad Sci USA. 2009; 106:15237–15242. [PubMed: 19720997]
19. D'Agostino VG, et al. Functional analysis of MUTYH mutated proteins associated with familial adenomatous polyposis. DNA Repair (Amst). 2010; 9:700–707. [PubMed: 20418187]
20. Kundu S, Brinkmeyer MK, Livingston AL, David SS. Adenine removal activity and bacterial complementation with the human MutY homologue (MUTYH) and Y165C, G382D, P391L and Q324R variants associated with colorectal cancer. DNA Repair (Amst). 2009; 8:1400–1410. [PubMed: 19836313]
21. Porello SL, Leyes AE, David SS. Singleturnover and presteadystate kinetics of the reaction of the adenine glycosylase MutY with mismatchcontaining DNA substrates. Biochemistry. 1998; 37:14756–14764. [PubMed: 9778350]
22. Rich RL, Myszka DG. Higherthroughput, labelfree, realtime molecular interaction analysis. Anal Biochem. 2007; 361:1–6. [PubMed: 17145039]
23. Profrock D, Prange A. Inductively coupled plasmamass spectrometry (ICPMS) for quantitative analysis in environmental and life sciences: a review of challenges, solutions, and trends. Appl Spectrosc. 2012; 66:843–868. [PubMed: 22800465]
24. Pheeney CG, Arnold AR, Grodick MA, Barton JK. Multiplexed electrochemistry of DNAbound metalloproteins. J Am Chem Soc. 2013; 135:11869–11878. [PubMed: 23899026]
25. Boon EM, Salas JE, Barton JK. An electrical probe of protein–DNA interactions on DNAmodified surfaces. Nat Biotechnol. 2002; 20:282–286. [PubMed: 11875430]
26. Kelley SO, Barton JK, Jackson NM, Hill MG. Electrochemistry of methylene blue bound to a DNA-modified electrode. Bioconjug Chem. 1997; 8:31–37. [PubMed: 9026032]
27. Pope MA, David SS. DNA damage recognition and repair by the murine MutY homologue. DNA Repair (Amst). 2005; 4:91–102. [PubMed: 15533841]
28. Johnson MK, Duderstadt RE, Duin EC. Biological and synthetic [Fe_3S_4] clusters. Adv Inorg Chem. 1999; 47:1–82.
29. Sweeney WV, Rabinowitz JC. Proteins containing 4Fe4S clusters: an overview. Annu Rev Biochem. 1980; 49:139–161. [PubMed: 6250442]
30. Duff JLC, Breton JLJ, Butt JN, Armstrong FA, Thomson AJ. Novel redox chemistry of [3Fe4S] clusters: Electrochemical characterization of the allFe(II) form of the [3Fe4S] cluster generated reversibly in various proteins and its spectroscopic investigation in *Sulfolobus acidocaldarius* ferredoxin. J Am Chem Soc. 1996; 118:8593–8603.
31. Netz DJA, et al. Eukaryotic DNA polymerases require an iron–sulfur cluster for the formation of active complexes. Nat Chem Biol. 2012; 8:125–132.
32. Good NE, et al. Hydrogen ion buffers for biological research. Biochemistry. 1966; 5:467. [PubMed: 5942950]
33. Ugwu SO. The effect of buffers on protein conformational stability. Pharm Technol. 2004; 28:86–108.
34. Kundu S, Brinkmeyer MK, Eigenheer RA. Ser 524 is a phosphorylation site in MUTYH and Ser 524 mutations alter 8oxoguanine (OG): a mismatch recognition. DNA Repair (Amst). 2010; 9:1026–1037. [PubMed: 20724227]
35. Dorn J, Ferrari E, Imhof R, Ziegler N, Hubscher U. Regulation of human MutYH DNA glycosylase by the E3 ubiquitin ligase mule. J Biol Chem. 2014; 289:7049–7058. [PubMed: 24443563]
36. Asso M, Guigliarelli B, Yagi T, Bertrand P. EPR and redox properties of *Desulfovibrio vulgaris* Miyazaki hydrogenase: comparison with the Ni–Fe enzyme from *Desulfovibrio gigas*. Biochim Biophys Acta. 1992; 1122:50–56. [PubMed: 1321673]
37. Kowal AT, et al. Effect of cysteine to serine mutations on the properties of the [4Fe4S] center in *Escherichia coli* fumarate reductase. Biochemistry. 1995; 34:12284–12293. [PubMed: 7547971]
38. Golinelli MP, Chmiel NH, David SS. Sitedirected mutagenesis of the cysteine ligands to the [4Fe-4S] cluster of *Escherichia coli* MutY. Biochemistry. 1999; 38:6997–7007. [PubMed: 10353811]

39. Bai H, et al. Functional characterization of two human MutY homolog (hMYH) missense mutations (R227W and V232F) that lie within the putative hMSH6 binding domain and are associated with hMYH polyposis. Nucleic Acids Res. 2005; 33:597–604. [PubMed: 15673720]

40. Ali M, et al. Characterization of mutant MUTYH proteins associated with familial colorectal cancer. Gastroenterology. 2008; 135:499–507. [PubMed: 18534194]

41. Bai H, et al. Functional characterization of human MutY homolog (hMYH) missense mutation (R231L) that is linked with hMYHassociated polyposis. Cancer Lett. 2007; 250:74–81. [PubMed: 17081686]

42. Goto M, et al. Adenine DNA glycosylase activity of 14 human MutY homolog (MUTYH) variant proteins found in patients with colorectal polyposis and cancer. Human Mutat. 2010; 31:E1861–1874.

43. Fleischmann C, et al. Comprehensive analysis of the contribution of germline MYH variation to earlyonset colorectal cancer. Int J Cancer. 2004; 109:554–558. [PubMed: 14991577]

44. Luncsford PJ, et al. A structural hinge in eukaryotic MutY homologues mediates catalytic activity and Rad9Rad1Hus1 checkpoint complex interactions. J Mol Biol. 2010; 403:351–370. [PubMed: 20816984]

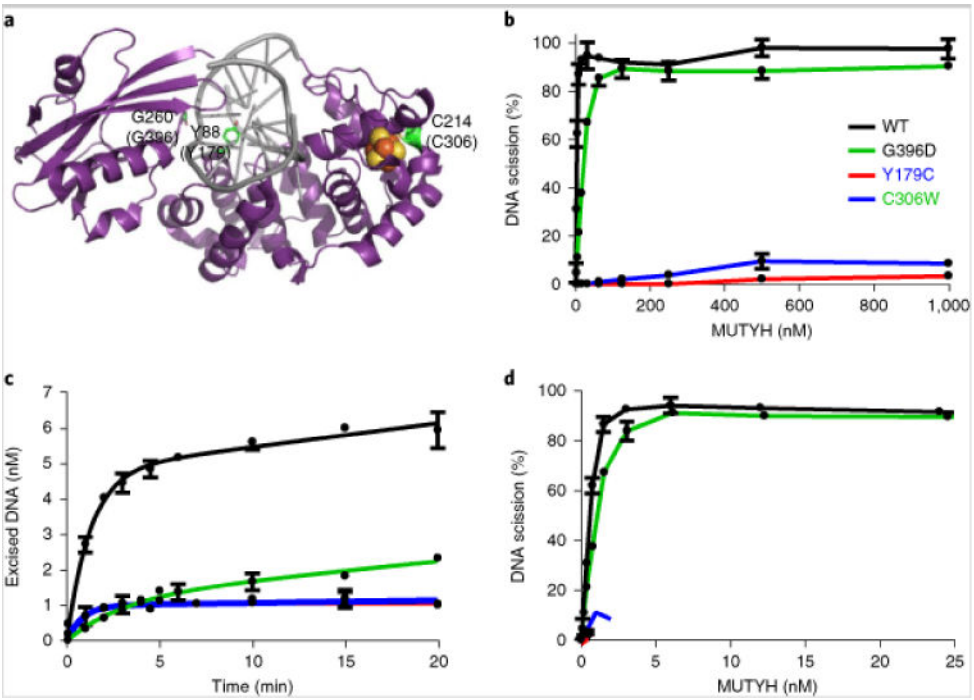

Fig. 1.

A novel human MUTYH variant, C306W, lacks glycosylase activity.

a, Ribbonmodel structure of MutY/DNA complex illustrating two pathogenic, well-characterized MAPrelevant residues Y179C and G396D, as well as the newly identified variant C306W. All three amino acids are conserved from bacteria to humans. Their relative positions are illustrated using a *Geobacillus stearothermophilus* MutY/DNA complex, with the corresponding residue numbers from human MUTYH isoform β3 in parentheses (structure from PDB ID 1RRQ). The novel C306W mutation occurs in one of four cysteine residues that ligate the conserved [4Fe4S] cluster in MUTYH. Black lines, wildtype MUTYH; green lines, G396D; red lines, Y179C; blue lines, C306W. All data are presented as mean+s.d., n=3. **b**, Glycosylase assay using soluble, monomeric MUTYH. Relative to WT and G396D MUTYH, Y179 and C306 proteins demonstrate severely attenuated DNA scission activity. **c**, Multiple turnover reaction conditions define the concentration of active protein within a purified protein sample. The glycosylase assay was performed with sufficient MUTYH protein to generate reaction burst amplitudes (A_o) within the detectable range. MUTYH active fractions, A_o, and k_B and k_L rate constants of the excision reaction during the exponential and linear phase, respectively, were determined by fitting the data points to the equation $[P]=A_o[1-\exp(-k_B)t]+k_L t$. **d**, Adenine excision activity of WT and mutant MUTYH proteins after correcting for active fractions, A_o. The correction for active MUTYH C306W and Y179C proteins shifted their assay concentrations below 2.5nM.

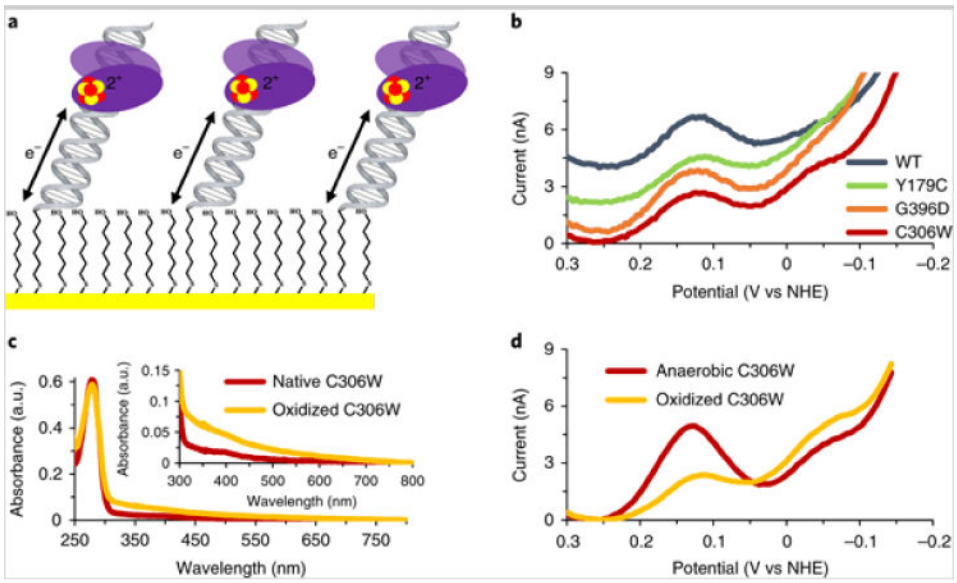

Fig. 2.

Initial electrochemical and spectroscopic characterization of MUTYH variants.

a, Electrochemistry is carried out on DNAmodified gold electrodes, which allow controlled reduction or oxidation of the [4Fe4S] cluster. **b**, Incubation of 2–2.5μM WT, Y179C, G396D or C306W MUTYH on a DNAmodified electrode in storage buffer (20mM Tris, 100mM NaCl, 1mM dithiothreitol (DTT), 0.5mM EDTA, 10% glycerol vol/vol, pH7.4) resulted in a reversible signal with a midpoint potential of ~105mV versus NHE. C306W uniquely exhibited an irreversible reductive peak around −50 mV versus NHE, which we presumed to be some form of oxidative degradation product. **c**, After aerobic oxidation by bulk electrolysis, the UV–vis spectrum of C306W showed no evidence of aggregation but did display a broad increase in absorption from 700 to 300nm, suggestive of cluster oxidation. **d**, Consistent with cluster degradation in the presence of oxygen, aerobic bulk electrolysis of C306W enhanced the size of the irreversible peak relative to the reversible signal, while anaerobic incubation provided a protective effect. All square wave voltammetry (SQWV) measurements were obtained at a frequency of 15Hz and 0.025V amplitude, and the signals shown are an average from at least four separate electrodes on a multiplexed chip. The SQWV background current levels in **b** were all comparable and have been adjusted for ease of visualization. Bulk electrolysis was performed for 1h at 0.412V versus NHE on a DNA-modified gold rod electrode in a glass cell.

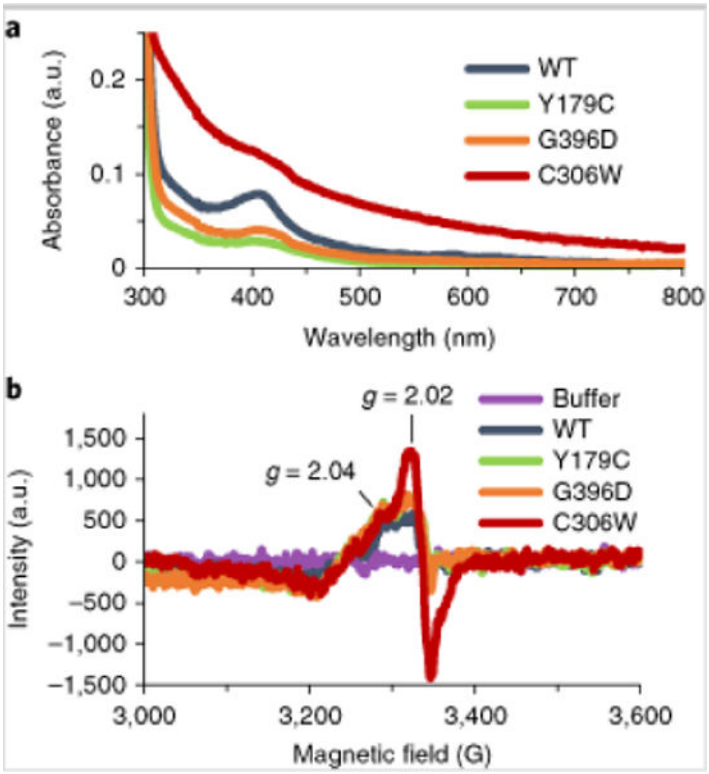

Fig. 3.

Characterization of MUTYH in HEPES and analysis of the C306W decay product.

a, UV–vis spectra of concentrated WT, Y179C and G396D exchanged into HEPES buffer (20mM HEPES, 100 mM KCl, 1mM DTT, 0.5mM EDTA, 10% glycerol vol/vol, pH7.4) all displayed the characteristic [4Fe4S] cluster absorption band centred at 410nm. In contrast, the C306W spectrum showed broadly increased absorbance associated with oxidation. **b**, EPR spectra of 15μM (WT and C306W) or 5μM (Y179C and G396D) MUTYH variants. The C306W EPR spectrum shows a sharp peak at g=2.018 with a shoulder at g=2.04, supporting identification of the degradation product as a $[3Fe4S]^{+}$ cluster. Continuouswave Xband EPR spectra were measured at 10K with 12.88mW microwave power, 2G modulation amplitude, and 5.02×10^{3} receiver gain.

Table 1

Determination of rate and binding constants

Multiple turnover experiment					
Enzyme ID	**[Protein] (nM)**	**A_0**	**A_0/[protein] (%)**	**k_B (min^{-1})**	**k_L (min^{-1} nM)**
Wild type	25	4.8±0.2	19.2	0.8±0.1	0.07±0.01
Y179C	2,670	1.1±0.1	0.04	1.0±0.2	0
C306W	500	1.0±0.1	0.2	1.2±0.2	0.01±0.01

Multiple turnover experiment					
Enzyme ID	**[Protein] (nM)**	***A***	***A*/[protein] (%)**	***k* (min)**	***k* (min nM)**
G396D	25	1.2±0.2	4.9	0.3±0.1	0.05±0.01
Enzyme/DNA kinetic binding data obtained from biolayer interferometry					
Enzyme ID	**k_{on} ($M^{-1}s^{-1}$) ×10^4**	**k_{off} ($10^{-4}s^{-1}$)**	**K_D (10^{-9}M)**		
Wild type	43±0.4	2.7±0.03	0.6±0.01		
Y179C	2.9±0.4	5.0±0.21	17±2.57		
C306W	No binding				
G396D	10±0.5	5.3±0.12	5.2±0.27		

Top: Determination of rate constants from multiple turnover experiment.

Bottom: Determination of binding constants with BLI. k and k are the association and dissociation rates and K is the equilibrium dissociation constant.

Data show mean+s.d., n=3.

Top: Determination of rate constants from multiple turnover experiment.

Bottom: Determination of binding constants with BLI. k_{on} and k_{off} are the association and dissociation rates and K_D is the equilibrium dissociation constant.

Data show mean+s.d., n=3.

Table 2

Elemental iron analysis of MUTYH proteins by ICPHRMS

Enzyme ID	[Fe] (μM)	[MUTYH] (μM)	Ratio 4Fe/enzyme (%)
Wild type	6.42±0.32	1.36	115
Y179C	6.40±0.32	1.65	95
C306W	0.78±0.03	1.63	9
G396D	6.59±0.33	1.62	99
Buffer	0.17±0.03		

Data show mean±s.d., n=3.

Table 3

Midpoint potentials of MUTYH and mutants as measured by CV

MUTYH variant	E_{mdpt} in Tris (mV)	E_{mdpt} in HEPES (mV)
WT	106±1	93±1
C306W	114±3	97±1
Y179C	105±0.8	100±2
G396D	115±0.1	99±4

Potentials are the average of at least three independent measurements, and error is s.d. of the mean.